The imprint of windblown dust from the North American Southwest on the California Channel Islands and Pacific Ocean sediments

Jardine. G.E.[a], Crocker A.J. [a,], Bailey, I. [b], Cooper, M.J. [a], Milton, J.A. [a], and Wilson, P.A.[a]

[a] University of Southampton, Waterfront Campus, National Oceanography Centre, Southampton SO14 3ZH, UK

[b] Cambourne School of Mines and Environment and Sustainability Institute, University of Exeter, Penryn Campus, Cornwall, UK

Corresponding Authors: A.J. Crocker. Email address: anya.crocker@noc.soton.ac.uk, P.A. Wilson Email address: paw1@noc.soton.ac.uk

Keywords: Present, Quaternary, Paleoclimatology, North America, Radiogenic isotopes

Abstract

Climate projections for the North American Southwest (NASW) predict an increasing frequency and duration of droughts over the 21st century in response to human-induced warming, with potentially severe economic and social consequences. The geological record provides a way to contextualise this prediction because of the past occurrence of abrupt hemispheric warming events and sustained intervals of atmospheric carbon dioxide loading equivalent to those projected for AD 2100 (between ~500 and 900 ppmv). Yet, terrestrial climate archives are typically too short and incomplete to provide a full record of these events. In principle, drill cores from deep sea sediments in the eastern Pacific Ocean can be used to

overcome this problem because they contain long records of continental dust and distal riverine-supplied sediments from North America. Yet our limited understanding of the provenance and transport pathways of these sediments impedes use of these marine archives for this purpose. Here we present radiogenic isotope data (Sr, Nd and Pb) from known NASW dust-producing hot spots – playa lakes in the Mojave Desert, Quaternary silts mantling the California Channel Islands and the terrigenous fraction from marine sediments of the eastern Pacific Ocean, supported by new maps of bedrock isotopic composition in the NASW. We use these and published data sets to infer the origin of playa lake silts in the Mojave Desert and the source of windblown sediments to the California Channel Islands and nearby ocean basins. Our results rule out a significant contribution from the distal tails of either the Pacific Asian dust plume or the North African dust plume to the Quaternary Channel Island silt mantles, corroborating the suggestion that they are aeolian in origin and sourced from the NASW on the Santa Ana winds. We identify the Outer California Borderland basins as an attractive proposition for studying past dust flux and palaeoaridity in the North American Southwest.

1 Introduction

Climate projections to the year 2100 predict an increased frequency and duration of droughts in response to human-induced warming in mid-latitude arid to semi-arid regions (Ault et al., 2016; Balling and Goodrich, 2010; Cayan et al., 2010; Cook et al., 2015; Seager et al., 2007). In the North American Southwest (NASW; typically taken to include the states of California, Nevada, Utah, Colorado, New Mexico and Arizona, Figure 1a), these changes are already evident (Ault et al., 2016; Balling and Goodrich, 2010; Cook et al., 2015; Seager et al., 2007). The 2012-2016 Californian drought cost the agriculture industry an estimated $603 million and the loss of over 1,500 jobs in 2016 alone (Medellín--Azuara et al., 2016). There is a pressing need, therefore, to assess the robustness of model predictions for hydroclimate in this

46 region (Cook et al., 2015; MacDonald et al., 2008).

47 Past climate records help to ground-truth future climate projections and geological data
48 provide a way to extend beyond the modern observational record by reaching deeper into the
49 past to cover a greater range of past climate conditions. Dendrochronological reconstructions
50 document numerous multi-decadal 'mega' droughts during the past 2,000 years (Cook et al.,
51 2014; Cook et al., 2007; Salzer and Kipfmueller, 2005). Although long lasting and severe
52 (decadal in length, covering at least 50% of the North American west), these megadroughts
53 occurred when atmospheric carbon dioxide levels were substantially lower than today (~280
54 ppmv during the Medieval Warm Period, compared with ~415 ppmv, January 2021 (Ahn et al.,
55 2012; Keeling et al., 2001)) and only about one third as high as the levels predicted for 2100
56 under a 'business as usual' emissions scenario (>900 ppm under RCP 8.5 (Meinshausen et al.,
57 2011)). It is instructive, therefore, to reach deeper into the geological past, to study intervals that
58 incorporate the range of estimates for 21st century greenhouse gas levels such as the mid-
59 Piacenzian Warm Period (3.3-3 Ma) (e.g. de la Vega et al., 2020) and Miocene (e.g. Super et
60 al., 2018).

61 Lake sediments provide valuable archives of terrestrial hydroclimate in the NASW, including
62 records of variability in aeolian dust and plant leaf waxes (Feakins et al., 2014; Routson et al.,
63 2016; Tchakerian and Lancaster, 2002), but in dryland and arid-prone regions, lakes are short-
64 lived and age control can be challenging. To study pre-Quaternary palaeoclimate states, we turn
65 to marine sediment core archives, which have the potential to provide continuous, long, well-
66 dated records of terrestrial hydroclimate in deeper time (e.g. Rea, 1994; Tiedemann et al.,
67 1994). Mineral dust deposition in sediment cores can be used as a proxy for aridity in the
68 terrestrial source region because of the strong (but not necessarily simple) relationship between
69 precipitation and natural dust emissions (Hoell et al., 2014; Just et al., 2012; Larrasoana et al.,
70 2003; Nizou et al., 2011; Pettke et al., 2000; Pye, 1987b; Seo et al., 2015; Seo et al., 2014).

Yet, marine sediment cores may also receive terrestrial sediments sourced from rivers or ocean currents. Terrigenous flux to the marine realm cannot, therefore, always simply be interpreted as an indicator of aridity, even when those terrigenous sediments are sourced from regions that are dry today. To decipher better the climate record imprinted on sediment cores we need to distinguish between different terrigenous sources and different modes of delivery to the ocean.

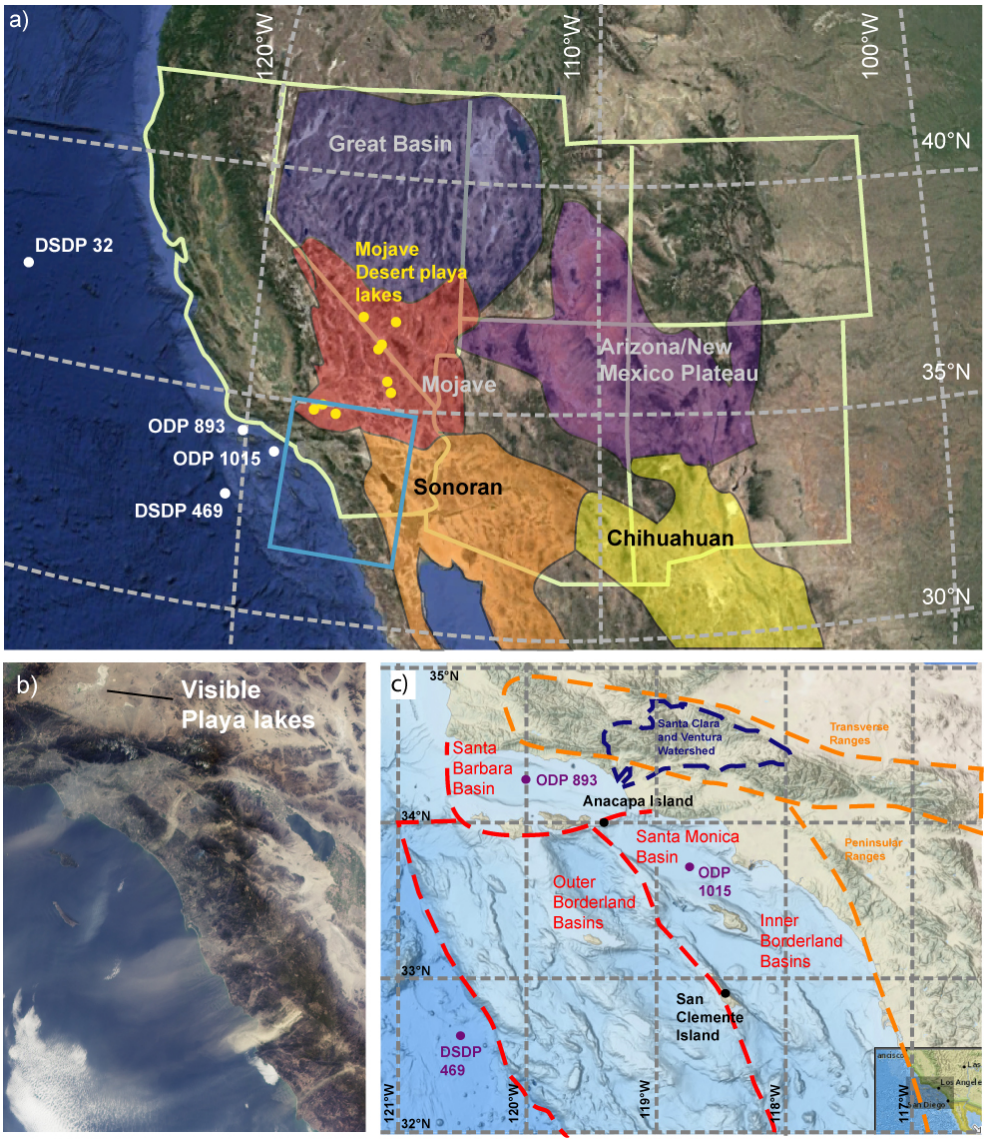

Figure 1 Study region with locations of new and previously published data reported herein: a) North American states typically included in the North American Southwest (NASW) (clockwise from left: California, Nevada,

Utah, Colorado, New Mexico, Arizona) with five major deserts highlighted (Google Earth imagery). Locations of DSDP sites 469 and 32, ODP sites 893 and 1015 and the sampled Mojave Desert playa lakes (yellow filled circles) also shown. Blue box in the lower left-hand corner denotes area shown in the next panel. b) MODIS Satellite imagery showing dust plumes transported over the Californian Borderland Basins by the Santa Ana wind system on 9th February 2002 (NASA, 2002). c) Map of southern California topography and offshore bathymetry showing location of Inner and Outer Borderland Basins, the coastal Transverse and Peninsular mountain ranges, the locations of ODP sites 893 and 1015 and locations of Anacapa and San Clemente Islands.

Radiogenic isotopes, particularly lead (Pb), neodymium (Nd) and strontium (Sr) are valuable tools to help distinguish between the provenance of sedimentary material accumulating in marine settings over a wide range of spatial and temporal scales (e.g. Abouchami and Zabel, 2003; Cole et al., 2009; Hyeong et al., 2011; Nakai et al., 1993; Pettke et al., 2000; Seo et al., 2014; Xie and Marcantonio, 2012). One particularly influential study of core-top sediments characterised pelagic clays delivered to the central and eastern Pacific Ocean as a mixture of three primary detrital components derived from continental source areas in Asia, Central and South America and North America (Stancin et al., 2006). The fidelity of these interpretations is weakened, however, by limited information on NASW sources.

Here we present (i) new radiogenic isotope data (Pb, Nd and Sr isotopic compositions) for dust source regions in the NASW, silt mantles from the Channel Islands offshore southern California and the detrital silicate fraction of young marine sediment samples from Ocean Drilling Program (ODP) sites 1015 and 893 (Figure 1a,c) and (ii) new maps of bedrock isotopic composition in the NASW. We use these new data, together with published data, to improve understanding of the geochemical fingerprints of terrigenous sediments transported to the Pacific Ocean from the North American continent.

2 Materials and Methods

2.1 Sample selection and description

To investigate the export of terrigenous sediments from North America to the Pacific Ocean from source to sink, we studied three main types of samples: silt mantles from two California Channel Islands (Anacapa and San Clemente) proposed to derive from airborne dust from the North American mainland (Muhs et al., 2007; Muhs et al., 2008), surface sediments from playa lakes located in the Mojave Desert and marine sediments from two ODP sites (1015 and 893) on the California margin (Figure 1a,c). ODP Site 1015 is located in the Santa Monica Basin (33º42.925'N, 118º49.185'W; Figure 1c) at 901 meters below sea level (mbsl); ODP Site 893 is located in the Santa Barbara Basin (34º17.25'N, 120º02.19'W; Figure 1c) at 576.5 mbsl. The Mojave Desert and island samples were obtained from the United States Geological Survey (USGS), Colorado (courtesy of D. Muhs).

The Channel Island silt mantles are described by Muhs et al. (2007, 2008) as massive, silt-rich horizons that resemble loess, or aeolian silt, ranging from 2 to 30 cm thick, which contrast sharply with the lower subsoil. Precise dating of the silt mantles on San Clemente is difficult but they drape the youngest marine terrace which gives a maximum age of ~80 ka, although they could possibly be younger than 3 ka, based upon a single radiocarbon data point (Muhs et al., 2007). Mineralogical, geochemical and grain size profile measurements (Muhs et al., 2007; Muhs et al., 2008) suggest that the dominant source of the island silt mantles is from the North American continent (not from the island bedrock), implying a windblown origin, but the influence of an Asian dust source (Muhs et al., 2007) and perhaps the Sahara cannot be ruled out. Muhs et al. (2007) and Muhs et al. (2008) also report that the geochemical fingerprint of the fine fraction (< 2 μm; clay) in these silt mantles differs slightly from that of the coarser (2-53 μm; silt sized) fraction of the samples, hinting that the silts and clays within the silt mantles may have

126 different provenances. The identity of the North American source is equivocal – both the Mojave
127 Desert and the coastal Transverse and Peninsular mountains of Southern California have been
128 considered as potential source regions for this wind-blown material (Muhs et al., 2007; Muhs et
129 al., 2008).

130 To better characterise sources of aeolian supply to the Californian borderland from the
131 interior of the North American continent we targeted silts from the playa lakes of the Mojave
132 Desert. Playa lake and river valley sediments are known to be active sources of silt-sized
133 material for deflation and aeolian transport in dry conditions (Pye, 1987b) and offshore dust
134 transport on the Santa Ana winds that blow from the inland deserts through the mountian
135 passes of Southern California in response to high pressure systems over the Great Basin can
136 be observed in satellite imagery (Muhs et al. 2007, Figure 1b).

137 In addition to wind-borne transport of lithogenic material, the Santa Barbara and Santa
138 Monica basins also receive fluvial sediment eroded and transported by the Santa Clara and
139 Ventura River systems from the Transverse Ranges (Figure 1c), with the Santa Clara River
140 system supplying more than three times the amount of riverine material to the Santa Barbara
141 and inner borderland basins as the next largest source (Inman and Jenkins, 1999). We sampled
142 sediments of Holocene and deglacial age from ODP sites 1015 and 893 (locations Figure 1c) to
143 fingerprint these fluvial inputs. “Riverine” samples were selected to characterise the isotopic
144 composition of fluvially derived sediments delivered to the offshore borderland basins from the
145 Californian coastal river valleys during the Late Quaternary. These consist of macroscopically
146 obvious turbidites ultimately originating from fluvial sources at Site 1015 and conspicuous cm-
147 scale ‘grey-layers’ inferred to represent fine-grained flood deposits at Site 893 (Behl, 1995;
148 Marsaglia et al., 1995). “Hemipelagic” samples were also selected at ODP Site 1015, targeting
149 intervals of background sedimentation in between the event horizons.

2.2 Isotopic analyses

The Channel Island silt mantle sediments were sieved to remove the >63 μm fraction, following Muhs et al. (2007, 2008). A subset of these samples was also sieved over a fine mesh to isolate the <10 μm fraction to allow comparison with long-range transported Asian material. Prior to full chemical digestion, carbonates, organic material, biogenic silica and Fe-Mn oxides were removed from the fine fraction of the sieved Channel Island samples and bulk Mojave Desert playa lake silts and Californian borderland ODP sediment samples by a series of chemical preparation steps, adapted from Bayon et al. (2002). Approximately 5 g of dry bulk sediment was placed in sealable Nalgene conical flasks. A solution of ~10-25% acetic acid solution was used to decarbonate the samples, and then 10% hydrogen peroxide solution at 60°C was used remove organic matter. Biogenic silica was removed from the Channel Island silt mantles and California borderland ODP sediments using a 1.5M NaOH solution following the method of Povea et al. (2015). Fe and Mn oxides were removed from the silt mantle and borderland basin sediments using a 0.05 M hydroxylamine hydrochloride – 15% acetic acid – 0.03 M Na-EDTA solution buffered to pH4 with analytical grade NaOH in two steps: an initial three hour reaction period; followed by the replacement of the reagent with fresh solution and a second reaction period of 24 hours. For both these steps, the samples were left on a shaker table. For the Mojave Desert playa lake samples, the Fe-Mn removal step was not deemed necessary because tests showed no significant isotopic effect from an anthropogenic contribution of Pb from a subset of samples processed with a Fe-Mn oxide removal step.

For Pb, Nd and Sr isotopic analyses, the chemically processed sediment samples were freeze-dried and approximately 50 mg of freeze-dried sample was weighed into 15 ml Teflon pots. The samples were treated with a final additional cleaning step of 1M ammonium acetate solution following Pettke et al. (2000). Concentrated hydrofluoric acid (HF, ~27M) and concentrated nitric acid (HNO_3, ~12M) were added in a 5:1 ratio and the pots left to reflux at

~130°C for 48 hours. Pb and Nd were then separated from the digested mother solution by ion exchange column procedures and ion selective resin for Sr. Where necessary, a modified column sequence with an additional ion exchange column was used to enhance the separation of Ba from the Sr fraction. Average digestion blanks for Pb, Nd and Sr were 320 pg, 160 pg and 7 ng respectively. One digestion blank (affecting five samples) contained an anomalous concentration of Pb and was excluded from this calculation but review of the data from those five samples indicates no obvious offset from the remainder of the dataset, (see Supplementary Figure 1), so they are included herein. Average column blanks for Pb, Nd and Sr were 168 pg, 2 pg and 13.5 pg respectively. The Nd-isotope ($^{143}Nd/^{144}Nd$) and Pb-isotope ratios ($^{206}Pb/^{204}Pb$, $^{207}Pb/^{204}Pb$ and $^{208}Pb/^{204}Pb$) of the samples were measured at the University of Southampton using a multi-collector inductively coupled plasma mass spectrometer (MC-ICP-MS, Thermo Scientific Neptune). Pb isotopic compositions were analysed using the double spike method of Taylor et al. (2015). The average values of NIST 981 were 16.9394 ± < 0.0025, 15.4955 ± < 0.0026 and 36.7093 ± < 0.0078 for $^{206}Pb/^{204}Pb$, $^{207}Pb/^{204}Pb$ and $^{208}Pb/^{204}Pb$ respectively. Nd isotopic compositions were adjusted to a $^{146}Nd/^{144}Nd$ value of 0.7219 (Vance and Thirlwall, 2002). Mass-bias corrected ratios were normalized to the given $^{143}Nd/^{144}Nd$ value (0.512115) of the standard JNdi-1 (Tanaka et al., 2000). The average value of JNdi-1 run as unknowns were 0.512114 ± < 0.000006. $^{143}Nd/^{144}Nd$ ratios are reported in epsilon notation:

$$\varepsilon_{Nd} = \left(\frac{^{143}Nd/^{144}Nd_{sample}}{^{143}Nd/^{144}Nd_{CHUR}} - 1 \right) * 10^4 \quad (1)$$

where $^{143}Nd/^{144}Nd_{CHUR}$ is the Chondritic Uniform Reservoir value of 0.512638 (Jacobsen and Wasserburg, 1980).

The $^{87}Sr/^{86}Sr$ isotopic composition of the samples was measured at the University of Southampton using a thermal ionization mass spectrometer (Thermo-Fisher TRITON Plus) with

197 an ^{88}Sr beam of 2V. Fractionation was corrected using an exponential correction normalised to
198 $^{86}Sr/^{88}Sr = 0.1194$. NIST 987 was run as a reference standard, with a long-term mean value of
199 0.710243 ± 0.000021 (2σ) reported from repeat analyses on this instrument.

200 **2.3 Radiogenic isotope base maps**

201 To place our data and the published radiogenic isotope datasets of NASW dust sources into
202 a regional context we developed Pb, Nd and Sr isotope maps of the bedrock geology by
203 compiling published measurements from the scientific literature (full reference list is given in
204 Supplementary Information). Most of the data used to develop these maps are for whole rock
205 samples, but for some data accessed through the North American Volcanic and Intrusive Rock
206 Database (NAVDAT, navdat.org), this information was not available.

207 All data were assigned latitude and longitude coordinates using published site location
208 information in conjunction with Google Earth (format X°X'X''). The location information was then
209 converted to decimal degrees and input into MATLAB_R2017a. A subset of the latitude and
210 longitude coordinates was derived by generating a path function within Google Earth and using
211 the MATLAB script kml_shapefile.m (Toomey, 2010) to convert the resulting .kml file to a
212 MATLAB shape file that contained the coordinate information.

213 To generate the colour-shaded map background, the geo-referenced data were averaged
214 into 0.125°x0.125° latitude/longitude grid squares within the bounds of 110 to 125ºW and 30 to
215 40ºN. This irregularly spaced data set of grid-square-averaged isotope data points was used to
216 generate a regularly spaced 3D gridded data set, with the x and y coordinates given by the
217 latitude and longitude, and the z coordinate the associated isotopic value using the function
218 griddata.m. This function generated an isotopic 'data' value for the empty spaces in the original
219 data distribution using a natural interpolation function. Some samples of granitoid rocks have

much more radiogenic Sr values than typical rocks in the NASW, resulting in a skewed distribution of $^{87}Sr/^{86}Sr$ bedrock data. As such, the grid-averaged dataset was filtered to exclude $^{87}Sr/^{86}Sr$ values > 0.7350 to distinguish regional trends free of extreme local effects. $^{206}Pb/^{204}Pb$ isotope values > 21 were also excluded for similar reasons. Original, unfiltered maps are shown in Supplementary Figure 2. The interpolation function does not allow for an extrapolation outside the area bounded by data points, resulting in some regions in the map that lack a colour-coded background. The gridded data set was converted to a coloured map display using the "griddata" and "meshgrid" functions and projected using an equidistant conic projection system. Vector files of the North American coastline, rivers, and lakes, and geotiff files of North American topography were imported from the public domain database Natural Earth (naturalearthdata.com).

3 Results and Discussion

3.1 Isotope composition of Mojave Desert dust hotspots

The Mojave Desert is an important dust-producing region that is under-characterized geochemically (Urban et al., 2018). Our new Nd, Sr and Pb data for Mojave Desert playa lake silts (Figure 2) improve upon existing datasets, particularly by providing a Pb isotopic characterisation. The Mojave Desert playa lake silt samples that we analysed display a modest range in Pb isotope compositions of 18.722 to 19.362 for $^{206}Pb/^{204}Pb$; internal errors are ≤ ± 0.00023. ε_{Nd} values range from -7.5 to -12.0 (internal errors are ≤ ± 0.13 epsilon units) with the bulk of the distribution falling between -8.7 and -10.4 and relatively non-radiogenic $^{87}Sr/^{86}Sr$ ratios, ranging from 0.709447 to 0.716889; internal errors are ≤ ± 0.000104.

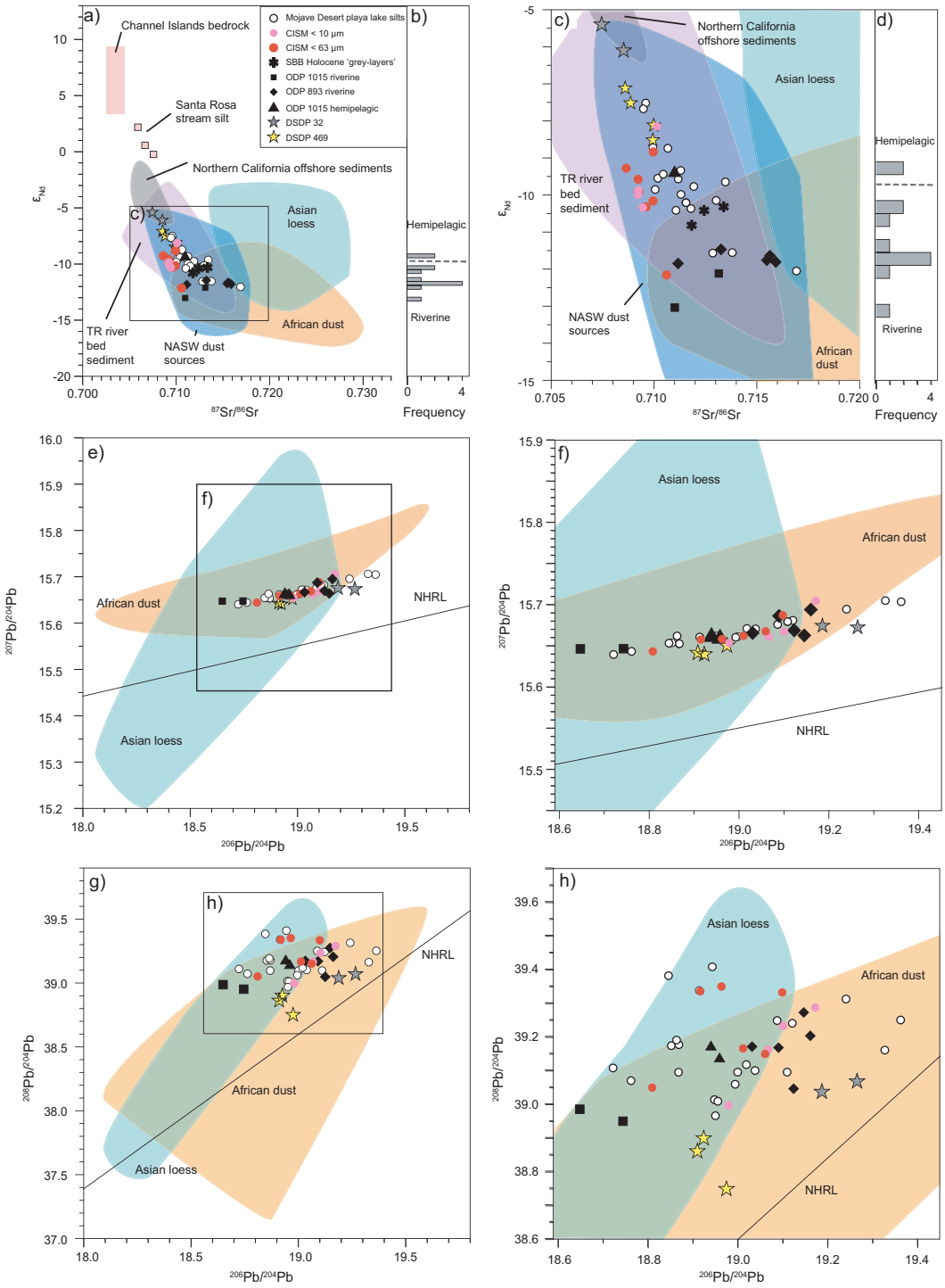

241

242 Figure 2 Radiogenic isotope characterisation of sources and sinks of windblown material from the NASW

and nearshore eastern Pacific Ocean in: (a-d) Nd-Sr space, (e-f) $^{206}Pb/^{204}Pb$ vs $^{207}Pb/^{204}Pb$ space and (g-h) $^{206}Pb/^{204}Pb$ vs $^{208}Pb/^{204}Pb$ spaces. Panel c) shows a close-up of the Nd-Sr region outlined in a) and panels b) and d) display histograms of the distribution of the ε_{Nd} isotope data from ODP sites 893 and 1015, distinguishing between 'riverine' and hemipelagic samples. Panel f) shows a close-up of the $^{206}Pb/^{204}Pb$ vs $^{207}Pb/^{204}Pb$ region outlined in e). Panel h) shows a close-up of the $^{206}Pb/^{204}Pb$ vs $^{208}Pb/^{204}Pb$ region outlined in g). Data for the NASW (in blue) and Transverse Ranges (TR) river sediment (in purple) (our data, Aarons et al., 2017; Napier et al., 2020) are compared to data from Chinese loess deposits, as representative of Asian dust sources (Chen et al., 2007; Jones et al., 2000; Kanayama et al., 2005; Sun and Zhu, 2010; Wu et al., 2011; Zeng et al., 2015; Zhao et al., 2015, in green) and trans-Atlantic African dust (Bozlaker et al., 2018; Kumar et al., 2014; Kumar et al., 2018; Meyer et al., 2011; Pourmand et al., 2014; Skonieczny et al., 2013; Skonieczny et al., 2011a; van der Does et al., 2018b, in orange). Data for the Channel Island silt mantles (this study), material from the California borderland basins from ODP sites 893 and 1015 and Pacific core data (this study, Napier et al., 2020; Rosenbauer et al., 2013; Stancin et al., 2006) indicate the isotopic composition of aeolian, riverine and hemipelagic sediments sourced from North America. Nd-Sr fields of the Channel Islands bedrock (Johnson and O'Neil, 1984; Weigand, 1993; Weigand and Savage, 1999) and stream bed material from Santa Rosa Island (Napier et al., 2020) are also shown in panel a). Key abbreviations: CISM = Channel Island silt mantles; SBB = Santa Barbara Basin. Northern Hemisphere Regression Line (NHRL) is shown on Pb isotope plots for reference (Hart, 1984).

3.1.1 Mojave playa lake silts versus bedrock signatures

Radiogenic isotopes are widely used to determine the provenance of terrigenous material deposited in marine sediments by comparing the isotope composition of the deposited sedimentary material to the continental bedrock and surface sediments in potential source regions upwind (e.g. Abouchami et al., 2013; Bailey et al., 2012; Lang et al., 2014). This approach commonly necessitates averaging bedrock compositions over large areas of heterogeneous geology (e.g. Lang et al., 2014; Walter et al., 2000). Our radiogenic maps allow us to test the fidelity of this approach. The geomorphology of the Mojave Desert is varied, both in its landforms and the geology of the country rocks (Baldridge, 2004; Jennings and Strand, 1981). Aeolian material from the Mojave Desert can therefore originate from a wide array of country rock lithologies. In Figure 3, we compare our bedrock isotope maps to our

measurements of the Mojave playa lake silts to assess similarities between proximal bedrock composition and aeolian material originating from the NASW. For all three isotope systems, our Mojave playa lake data fall within the range of the geological bedrock of the NASW region – for example, the $^{206}Pb/^{204}Pb$ isotopic composition of the geological bedrock ranges from approximately 17 to 20.5, which encompasses the spread of the measured $^{206}Pb/^{204}Pb$ values of the Mojave playa lake silts (~18.7 to 19.4). Some of the playas have very similar values to the local bedrock (Figure 3a-c), particularly in Pb and Nd space. The Sr isotope map (Figure 3c), however, clearly demonstrates that our samples from the playa lakes of the Mojave Desert are typically more radiogenic in $^{87}Sr/^{86}Sr$ than their underlying bedrock. This offset is of the correct sign to signal incongruent behaviour of rubidium (Rb) and Sr during weathering because that process typically gives rise to more radiogenic $^{87}Sr/^{86}Sr$ values in weathered sediments than in their parent bedrock (Dasch, 1969).

In summary, our Mojave Desert playa lake samples display a relatively narrow range in Pb, Nd and Sr isotopic composition when compared with the bedrock. The geochemistry and mineralogy of modern dust deposition in the Mojave indicates a well-mixed source of material (Reynolds et al., 2006), and the isotope characteristics of our playa lake samples are likely a function of this wide-scale mixing process across the desert. Next, we use these results to understand better the origin of the silt mantles on the Californian Channel Islands.

289

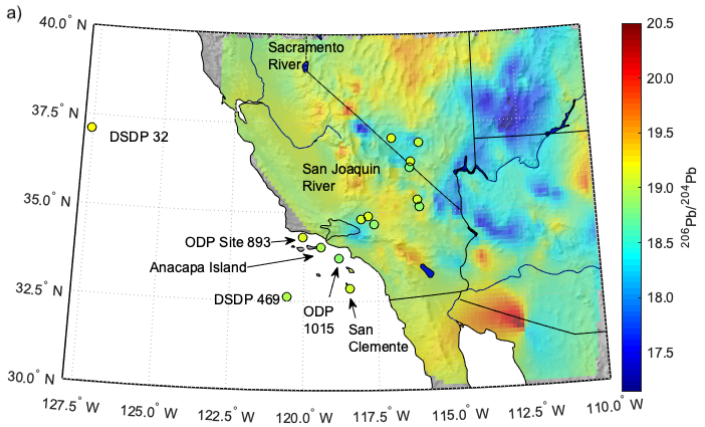

290

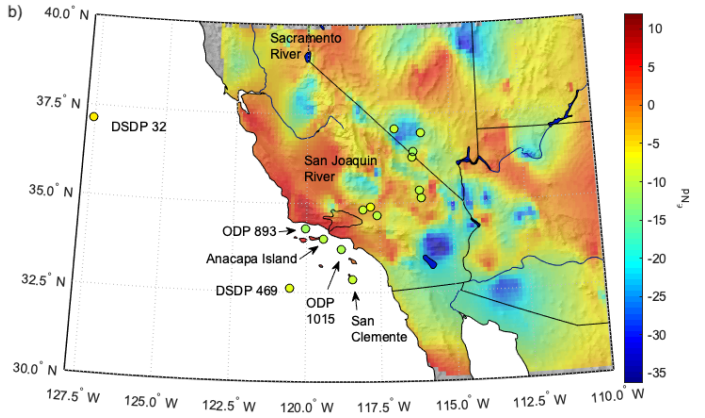

291

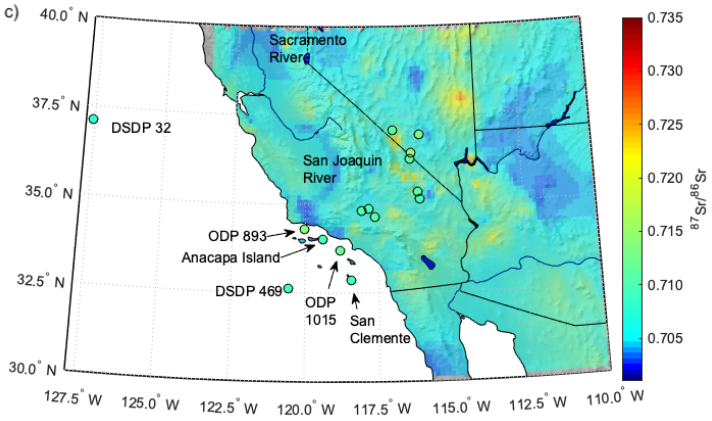

292 Figure 3 Radiogenic isotope maps of the bedrock geology of the North American Southwest (NASW) in
293 interpolated a) $^{206}Pb/^{204}Pb$; b) ε_{Nd}; c) $^{87}Sr/^{86}Sr$ space compared to data for unconsolidated sediment samples (this
294 study) from Mojave Playa Lake silts, Channel Island Silt Mantles, DSDP and ODP sites (coloured circles). Colour
295 scale (right) applies to both bedrock geology and sediment samples.

296 ### 3.2 Origin of Channel Island silt mantles, offshore Southern California.

297 #### 3.2.1 Assessing the likelihood of a significant local (island) source

298 Satellite imagery provides strong evidence for the transport of aeolian material to the
299 Channel Islands from the NASW (Figure 1b) but the importance of aeolian supply versus a local
300 contribution from the island bedrock to the silt mantles must be carefully assessed. Contrasting
301 bedrock lithology between the NASW and Channel Islands makes this a straightforward task.
302 For the <63 μm fraction of the Channel Island silt mantles (from San Clemente and Anacapa
303 islands) ε_{Nd} values range from -12.1 to -8.1 with internal errors ≤ ± 0.12 and $^{87}Sr/^{86}Sr$ ratios are
304 relatively non-radiogenic, ranging from 0.708610 to 0.710575 with internal errors ≤ ± 0.000083
305 (Figure 2a). The samples are closely grouped in Pb isotope space, from 18.809 to 19.098 in
306 $^{206}Pb/^{204}Pb$, from 15.644 to 15.677 in $^{207}Pb/^{204}Pb$ and from 39.051 to 39.337 in $^{208}Pb/^{204}Pb$ space
307 (internal errors ≤ ± 0.0063, 0.0058 and 0.0186, respectively; Figure 2e-h). The subset of
308 Channel Island silt mantle samples that are <10 μm have similar values in Pb isotope space to
309 the <63 μm fraction (Figure 2e-h). Their Nd isotopic values have a smaller range compared to
310 the <63 μm fraction and their average value is shifted to slightly more radiogenic (less negative)
311 ε_{Nd} values (-10.3 to -8.1, internal errors ≤ ± 0.07, Figure 2a). The measured $^{87}Sr/^{86}Sr$ values
312 (0.709194 to 0.710109, internal errors ≤ ± 0.000072, Figure 2a) of the <10 μm fraction fall within
313 the same range as the <63 μm fraction.

314 The isotopic values of these mantles are strikingly different to those of Channel Island
315 bedrock (Figure 2a). Whole-rock measurements of $^{87}Sr/^{86}Sr$ in San Clemente Island andesites
316 fall between 0.7037 and 0.7045 (Johnson and O'Neil, 1984). Although no bedrock Sr isotopic
317 data are available for Anacapa Island, these andesitic bedrocks are compositionally similar and
318 stratigraphically correlative to the volcanic suite on Santa Cruz Island (Weigand, 1993) which
319 has $^{87}Sr/^{86}Sr$ ratios from 0.7025 to 0.7032 (Johnson and O'Neil, 1984). Similarly, Nd isotope

data measured on the volcanics from the other Channel Islands (+3.4 to +9.4; Weigand and Savage (1999) and references therein) serve as a good guide for the base rock composition on Anacapa and San Clemente. Our data (Figure 2a) for the silt mantles contrast sharply with these island bedrock compositions (and even stream bed samples from Santa Rosa Island, Figure 2a, Napier et al. (2020)), providing strong support for the interpretations of Muhs et al. (2007) and Muhs et al. (2008) that the island silt mantles are aeolian in origin.

3.2.2 No significant input to Channel Island silts from Asia or Africa

Next, we consider potential external sources of the Channel Island wind-blown silts. We consider three main sources for this aeolian material: (i) the distal influence of the Pacific Asian dust plume bringing material predominantly originating from East Asia (Creamean et al., 2014; Uno et al., 2011; VanCuren and Cahill, 2002), (ii) aeolian material originating from Africa, considered because the Sahara is the world's largest dust source (Ginoux et al., 2012; Prospero et al., 2002) and African dust storms have been recorded travelling as far west as Colorado and Texas (Hand et al., 2017; Perry et al., 1997), or in very rare cases, eastwards across Asia and the Pacific to the western coast of North America (McKendry et al., 2007), and (iii) transport from North America on the Santa Ana winds (Figure 1b; Muhs et al., 2007; Muhs et al., 2008).

Comparison of similar size fractions helps to minimise the widely acknowledged effects exerted on $^{87}Sr/^{86}Sr$ by weathering and grain size (Dasch, 1969; Feng et al., 2009), with the fine silt- and clay-sized fractions of windblown material typically carrying higher $^{87}Sr/^{86}Sr$ ratios than their coarser fraction counterparts because of the preferential incorporation of K- and hence Rb-rich clay and mica minerals into the finest fractions (Feng et al., 2009). Although previous studies have shown that aeolian material transported over thousands of kilometres is borne largely in the <5 μm fraction (and often even in the <2 μm fraction (Pye, 1987a)), it is possible for larger dust particles to travel considerable distances from their source region (e.g. Betzer et

al., 1988; van der Does et al., 2018a) and the Channel Islands are <150 km from potential mainland US dust sources. Therefore, we consider data for the total suspended sediment, loess and where available, we include data measured on the <75 μm fraction. Taking this approach also accounts for the break of up larger-sized dust particles during saltation and other near-surface processes into finer size fractions and their subsequent long-range transport.

To evaluate the likelihood of an Asian influence we compare our data to measurements of Chinese loess deposits, which are representative of Asian-sourced dusts (Chen et al., 2007; Jones et al., 2000; Kanayama et al., 2005; Sun and Zhu, 2010; Wu et al., 2011; Zeng et al., 2015; Zhao et al., 2015), Figure 2. We find that the Pb isotope composition of Asian material is (Jones et al., 2000; Wu et al., 2011; Zeng et al., 2015) distinct from material originating on the North American continent (Figure 2e-h). The windblown island silt mantles and active North American dust sources cluster along a single, well-defined trend in $^{206}Pb/^{204}Pb$ vs $^{207}Pb/^{204}Pb$ space (Figure 2e-f) that is offset from the distribution of the Asian data field (Figure 2e-f). There is also minimal overlap in Nd-Sr space between the Asian data and the different sources of terrigenous material from the NASW (Figure 2a-c). Asian loess has a broader distribution in ε_{Nd} space (approx. -14 to -4) and typically shows much more radiogenic $^{87}Sr/^{86}Sr$ ratios than the Channel Island silts. In fact, the subset of Channel Island silt samples that were sieved to <10 μm do not overlap with the Asian loess in Nd-Sr space at all (Figure 2c). Thus, while Pb isotope data do not rule out the presence of Asian dust in the silt mantles when considered in isolation, when considered together with the Nd and Sr systems, radiogenic isotopes provide a powerful tool to distinguish more clearly between long-range transported Asian dust and North American-derived material (windblown and riverine) in Pacific sediments. Our data therefore clearly rule out the possibility of a major contribution from Asia to the windblown dust deposits accumulating on the California Channel Islands.

We next consider the likelihood of a significant deposition of trans-Atlantic African aeolian

material on the California Channel Islands by comparing our Channel Island silt mantle data to dust trap data from North Africa, the North Atlantic and the Caribbean (Bozlaker et al., 2018; Kumar et al., 2014; Kumar et al., 2018; Meyer et al., 2011; Pourmand et al., 2014; Skonieczny et al., 2013; Skonieczny et al., 2011b; van der Does et al., 2018b, Figure 2). While there is some overlap in Pb isotope space between our Channel Island data and the Saharan isotope fields (Figure 2e-h), there is little overlap in Sr-Nd isotope space. We also note that there is a poor isotopic match between the Channel Islands silt mantles and the two major North African regions implicated in trans-Atlantic dust transport: the western ($^{87}Sr/^{86}Sr$ = 0.7279±0.0052, ε_{Nd} = –14.8±2.2) and central ($^{87}Sr/^{86}Sr$ = 0.7186±0.0053, ε_{Nd} = –10±3.9) preferential source areas (Jewell et al., 2021). Therefore, we consider it unlikely that the Saharan dust plume makes a significant contribution to sediments offshore Southern California.

3.2.3 North American sources of Channel Island aeolian silt mantles

Next, we evaluate possible North American sources of dust. Both the Mojave Desert and the coastal mountains of Southern California are proposed as potential source regions of aeolian supply to the Channel Islands (Muhs et al., 2007; Muhs et al., 2008). Both of these regions contain playa lakes and river valleys, which are known sources of readily deflated silt-sized material (Pye, 1987b). We compare the Sr-Nd-Pb isotope composition of the Channel Island silt mantles to our Mojave playa lake silt data and other published records (Aarons et al., 2017; Napier et al., 2020) in Figure 2.

The <63 μm fraction of the Channel Island silt mantle samples shows a very similar trend in $^{206}Pb/^{204}Pb$ vs $^{207}Pb/^{204}Pb$ space to that of the Mojave playa lake silts (Figure 2e). In $^{206}Pb/^{204}Pb$ vs $^{208}Pb/^{204}Pb$ space, the <63 μm fraction of the Channel Island silt mantles are completely contained within the spread of the Mojave playa lake data (Figure 2g). Thus, on the basis of our Pb isotope data, the Mojave Desert is a compatible source for the aeolian material mantling the

Channel Islands. This conclusion is supported by the Nd isotope data because the composition of the Channel Island silt mantles is very similar to the Mojave Desert samples (Figure 2a,c). There is a slight discrepancy in Sr values between the Channel Island silts and the Mojave Desert playa lake silts (Figure 2c) but the Channel Island data fall within the spread of dust sources from the Mojave (Figure 2).

A geochemical characterization of the coastal mountains of southern California is provided by Napier et al. (2020) who sampled streambed sediments in the coastal California Transverse ranges (Figure 2a,c). There is extensive overlap in Sr-Nd space between the field described by those data and our data for the Mojave playa lakes and the Channel Island silt mantles (Figure 2). A study of potential dust sources across a wider area of the North American West shows that several other regions including the Colorado Plateau and Basin and Range province also show similar radiogenic isotope fingerprints to the Mojave (Aarons et al., 2017). Therefore, we cannot precisely identify the contribution to the island deposits made by each of these different source regions relative to the Mojave Desert. Regardless, our data strongly support the suggestion that these deposits are derived from North America (Muhs et al., 2007; Muhs et al., 2008) and the pathway of the Santa Ana winds across Southern California to the offshore Pacific (Conil and Hall, 2006; Hughes and Hall, 2010) suggests that active dust sources along this route, including those of the Mojave, are likely to be the most important contributors to the Channel Island silt mantles and surrounding ocean sediments.

3.3 Distinguishing sources of terrigenous deposition offshore Southern California

The Channel Island silt mantles provide an excellent case study to characterize the signature of aeolian material exported to the Eastern Pacific, but to find readily datable continuous palaeoclimate archives spanning many thousands or millions of years, we must turn

417 instead to marine deposits that can contain terrigenous inputs derived via both riverine and
418 aeolian transport.

419 Previous studies investigating sediment delivery to the California borderland basins
420 concluded that fluvial input dominates the sediment budget (>80% in some parts of the inner
421 borderlands, location Figure 1c); whereas biogenic material contributes typically 20-25% (Inman
422 and Jenkins, 1999; Schwalbach and Gorsline, 1985). However, more recent work points to a
423 significant additional input of aeolian material (Muhs et al., 2007). Although the predominant
424 transport direction of dust from the NASW is eastwards on westerly winds towards the North
425 American interior and possibly the distant Atlantic Ocean (Mahowald et al., 2006), at certain
426 times during autumn and winter, 'Santa Ana' winds carry dust westwards to the Pacific Ocean
427 ((Muhs et al., 2007; Muhs et al., 2008; Reheis et al., 1995) Figure 1b). It is estimated that
428 aeolian materials contribute anywhere between 5 and 60% of the sediment deposited in the
429 California Borderlands, which varies primarily as a function of dilution by riverine material and
430 biogenic inputs (Muhs et al., 2007). Here, we explore whether radiogenic isotopes can be used
431 to assess the relative importance of aeolian and fluvial inputs to the hemipelagic sediments at
432 ODP sites 893 and 1015.

433 To isolate the signature of the riverine inputs exported offshore Southern California, we
434 analysed samples from from marine drill cores at ODP sites 893 and 1015 containing fluvial
435 deposit horizons (the ODP Site 893 'grey-layers' and ODP Site 1015 turbidites). We compare
436 the radiogenic isotope composition of hemipelagic sediments from ODP Site 1015 (which
437 should contain both aeolian and riverine material) to these fluvially derived horizons and to the
438 Channel Island silt mantles to understand better the relative importance of these two sources to
439 hemipelagite formation in the region. The subset of our Californian margin borderland basin
440 samples (located in the Santa Barbara and Santa Monica basins (Figure 1c)) which are
441 dominantly fluvially derived have $^{87}Sr/^{86}Sr$ values between 0.710973 and 0.715886 (internal

errors ≤ ± 0.000007) and ε_{Nd} values between -13.0 and -11.4 (internal errors ≤ ± 0.14). The isotopic signatures of the fluvially derived layers in the Santa Barbara (ODP Site 893) and Santa Monica (ODP Site 1015) basins are very similar, with the samples from ODP Site 1015 recording slightly more unradiogenic ε_{Nd} and lower $^{206}Pb/^{204}Pb$ values (Figure 2) than ODP Site 893. Holocene and deglacial samples from ODP Site 1015 do not show an appreciable compositional difference attributable to age.

In Pb isotope space, the hemipelagic data are not offset from the fluvially sourced samples (Figure 2e-h), but Nd-Sr measurements of the ODP core samples (Figure 2a,c) indicate a subtle but quantifiable isotopic difference between horizons characterised as fluvial and 'hemipelagic background' (Kennett et al., 1994; Lyle et al., 1997). The ε_{Nd} values of the hemipelagic material (which is expected to contain both aeolian and fluvial inputs) are more radiogenic (-9.4 to -9.2; internal errors ≤ ± 0.08) than the fluvial samples (-13.0 to -11.4) and the $^{87}Sr/^{86}Sr$ composition plots at the less radiogenic end of the range in the riverine samples (Figure 2b-d).

The distinct isotopic composition of the hemipelagic sediments from ODP Site 1015 implies either a shift in the source of terrigenous material deposited in the absence of large fluvial inputs to the Santa Monica Basin or a mixing of the fluvial inputs with a second, isotopically distinct source of terrigenous material. Variability in the signature of the riverine inputs is supported by Napier et al. (2020), who attribute more radiogenic ε_{Nd} and less radiogenic $^{87}Sr/^{86}Sr$ values in sediment samples from the Santa Barbara Basin of Last Glacial Maximum age to an increased contribution from the southern slopes of the Santa Ynez and Topatopa Mountains. Alternatively, we note that hemipelagic sediment of both Holocene and deglacial age from ODP Site 1015 in the Santa Monica basin more closely resembles the Mojave Desert and Channel Island silt mantles than the dominantly fluvial material sampled at the same site in Nd-Sr space, supporting a greater influence of windblown dust from the NASW during times of hemipelagic deposition (Figure 2a).

In summary, we identify differences in Sr-Nd isotopic signatures between river-derived and hemipelagic sediments immediately offshore Southern California possibly attributable to differences in the geochemical signatures of aeolian and riverine sediments to the Californian margin. However, overlap between the isotopic signatures of terrestrial samples of source regions in the Mojave, Transverse Range and greater NASW mean that it is not yet possible to estimate the relative proportions of riverine and aeolian inputs to the Inner California Borderland Basins using Sr-Nd-Pb isotopes (Figure 2). We therefore suggest that the Outer California Borderland Basins are a more attractive proposition for studying past dust flux and palaeoaridity in the North American Southwest because inputs of riverine material there are much lower than to the Inner Borderland Basins (Schwalbach and Gorsline, 1985).

3.4 Spatial variations in the geochemistry of hemipelagic deposition in the Eastern Pacific

In their study of the provenance of terrigenous input to the Pacific Ocean, Stancin et al. (2006) analysed the lithogenic fraction from drill cores across the eastern Pacific to determine the relative contributions from Asia, South/Central America and North America. They identified two sediment core sites as containing a terrigenous fraction dominantly sourced from North America: Deep Sea Drilling Project (DSDP) sites 32 and 469. DSDP Site 469 is located at 32.61°N, south of ODP sites 893 and 1015, but it is further offshore than either of these two ODP sites, situated at the base of the Patton Escarpment bounding the Southern Californian Outer Borderland Basin (Figures 1 and 3). In contrast, DSDP Site 32 is located at 37.12°N, a similar latitude to San Francisco Bay, approximately 820 km north of DSDP Site 469 (Figure 3). Radiogenic isotope data of Plio-Pleistocene samples from these two sites were used to determine the North American end member in Pb, Sr and Nd space for the entirety of the North Pacific Ocean (Stancin et al., 2006). Our data provide a test of that approach.

3.4.1 North American terrigenous supply to the North Pacific Ocean

DSDP sites 32 and 469 are isotopically distinct from each other in Nd-Sr and Pb isotope space (Figure 2). DSDP Site 32 is located (Figure 3) proximal to the Delgada Submarine Fan (McManus et al., 1970), which consists of terrigenous material derived mainly from the San Joaquin and Sacramento river catchments and our Pb and Sr isotope maps show good isotopic agreement between the drainage basins of these two rivers (Figure 3, see also Supplementary Figure 2) and DSDP Site 32. Furthermore, there is good isotopic correspondence between the DSDP Site 32 data (Stancin et al., 2006) and sedimentary grab samples from the mouth and near offshore of San Francisco Bay where the San Joaquin and Sacramento Rivers enter the Pacific Ocean (Figure 2a, data labelled as 'Northern California offshore sediments' (Rosenbauer et al., 2013)). Taken together, these lines of evidence strongly suggest that the dominant source of the hemipelagic deposition at DSDP Site 32 is derived from fluvial supply from Northern California.

DSDP Site 469 is located well to the south of DSDP Site 32, just seaward of the Southern Californian Borderland basin system and the Channel Islands that lie therein (Figures 1 and 3). Here, the influence of Northern Californian rivers is suggested to be minimal (Griggs and Hein, 1980) and our analysis substantiates this suggestion because, in contrast to DSDP Site 32, the terrigenous fraction from DSDP Site 469 shows significant isotopic correspondence with Channel Island silts and NASW dust sources (Figure 2, this study, Aarons et al. (2017); Stancin et al. (2006)). These findings suggest that aeolian-sourced material from the NASW is a significant contributor to hemipelagic deposition at DSDP Site 469.

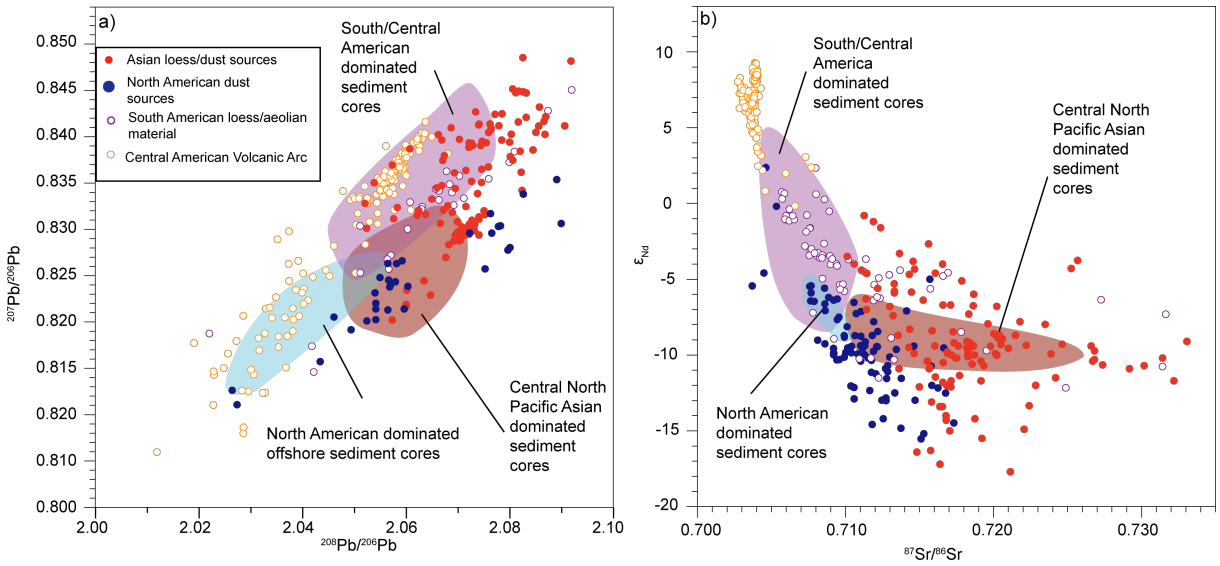

512

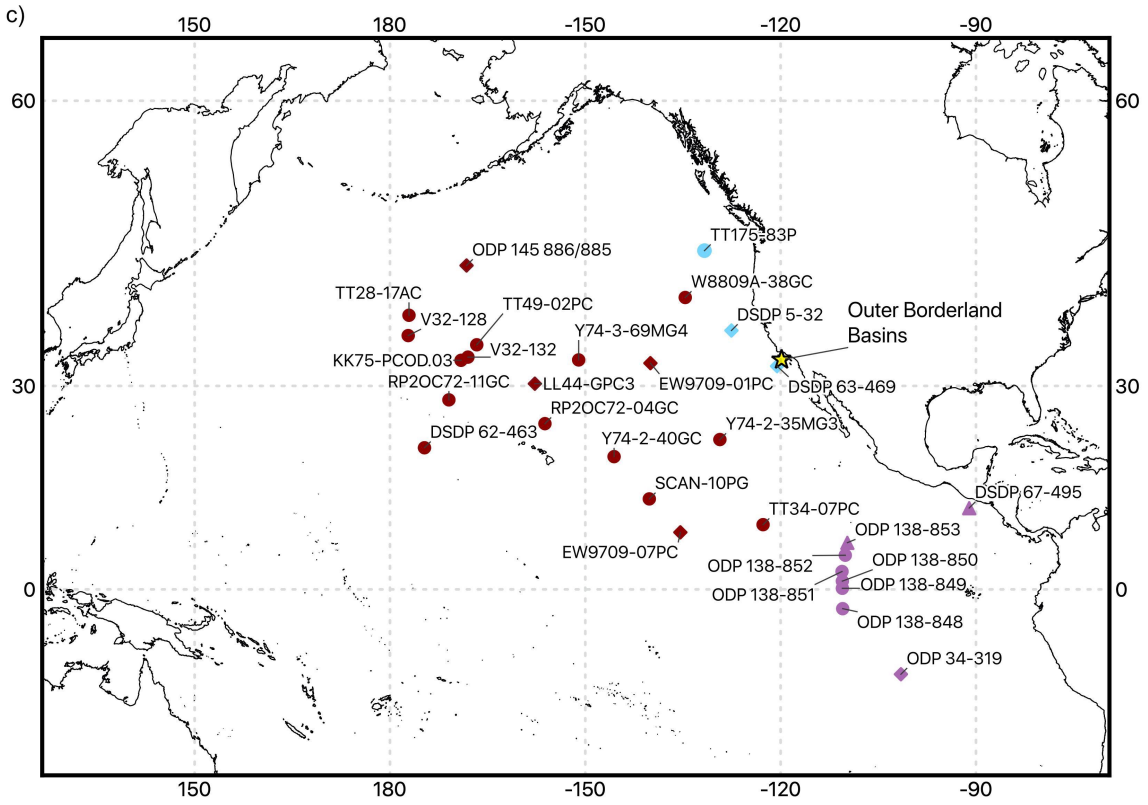

513

514 Figure 4 Radiogenic isotope characterisation of sources of Asian, South/Central American and North
515 American aeolian material compared to the radiogenic isotope signature recorded in eastern Pacific marine sediment
516 cores downwind of these continents in a) $^{208}Pb/^{206}Pb$ vs $^{207}Pb/^{206}Pb$ space and b) Nd-Sr space. Panel a) displays Pb

517 isotope ratios plotted as $^{208}Pb/^{206}Pb$ vs $^{207}Pb/^{206}Pb$ to be consistent with Stancin et al. (2006). The sediment cores are
518 grouped into three fields representing the dominant source as identified by Stancin et al. (2006). We have updated
519 these three isotopic fields to include new data from both the original sites and new ones. c) Locations of the Pacific
520 marine sediment cores used to characterize the radiogenic isotope fields displayed in panels a) and b). Colours of the
521 markers correspond to the interpreted dominant source of terrigenous material at that core site. Red = Asia; blue =
522 North America; purple = South/Central America. The marker shape indicates whether the data generated from that
523 sediment core were included in the analysis of Stancin et al. (2006). Diamonds = sediment cores for which we use
524 the same data as Stancin et al. (2006); triangles = sediment cores used by Stancin et al. (2006) with additional data
525 incorporated here; circles = sediment cores not included in Stancin et al. (2006). Note that Sr isotope data are not
526 included from ODP sites 848-851 due to the influence of marine barite on sediment signatures at these sites (Xie and
527 Marcantonio, 2012). Data sources are listed in the Supplementary Information. (For interpretation of the references to
528 colour in this figure legend, the reader is referred to the Web version of this article.)

529 In Figure 4 we compare the isotopic composition of the terrigenous fraction in Pacific Ocean
530 marine sediment cores with data from continental sediment sources, including our new data for
531 North America. The comparison shows much greater ranges in isotopic composition of the
532 sediment sources than the sediment sinks (the cores), highlighting the extent of signal
533 homogenisation in the marine core data caused by mixing of contributions during transport over
534 long distances.

535 Our comparisons clearly highlight the advantage of considering multiple isotope systems to
536 characterise and trace long-range aeolian transport and deposition. For example, there is
537 considerable overlap in Nd-Sr isotope space between North American sediment sources and
538 the South/Central American-dominated provenance grouping in the sediment core data (Figure
539 4b) but a major North American influence on the eastern equatorial Pacific can be ruled out by
540 the clear distinction in Pb isotope space illustrated in Figure 4a.

541 More work is needed to pinpoint the contributions of different dust sources in western North
542 America but our data provide a solid framework to help trace the extent and temporal variability

543 of North American dust deposition in the Pacific Ocean. Current data coverage in the Northeast
544 Pacific is sparse, with sites from both riverine and dust-dominated locations included in Figure
545 4. Detailed characterisation of the aeolian sediment source region signatures permits a more
546 accurate assessment of their long-range contributions than can be provided by marine
547 sediments where riverine and aeolian inputs from multiple sources commonly mix. Our results
548 support the use of radiogenic isotopes to discriminate between Asian and North American
549 sourced dusts in Pacific Ocean sediments. However, distinguishing aeolian inputs from riverine
550 supply along the Californian margin using radiogenic isotopes alone is not straightforward. We
551 suggest that future work on dust export from the NASW should focus on more sites in the Outer
552 California Borderland Basins and eastern Pacific margin where the influence of riverine supply
553 is smaller than for the Inner Borderland Basins.

554 # 4 Conclusions

555 We present new radiogenic isotope data to characterise sources and sinks of terrigenous
556 material originating from the North American Southwest in conjunction with new Pb, Sr and Nd
557 isotope maps of the geological bedrock of the region capturing the broad-scale features of
558 bedrock that help to trace sources and sinks of aeolian material. Our radiogenic isotope data
559 improve our ability to geochemically fingerprint terrigenous material (both aeolian and fluvial)
560 from the North American Southwest (NASW) and permit clear distinction between windblown
561 material from the NASW and long-range transported material from Asia and North Africa. We
562 rule out a significant contribution from either Asia or North Africa to the Quaternary silts mantling
563 the California Channel Islands and corroborate the suggestion that they are aeolian in origin and
564 sourced from the NASW on the Santa Ana winds.

565 We conclude that aeolian-sourced material from the NASW is a significant contributor to
566 marine sediments offshore Southern California. The geochemical distinction between riverine

and hemipelagic deposits reveals the potential of the sediments of the Outer California Borderland Basins to preserve a signature of past aeolian inputs and hence produce high-fidelity reconstructions of dust export and palaeoaridity in the NASW over geological timescales.

Acknowledgements

We thank D. Muhs at the USGS for samples and valuable insights during the course of this research. Sediment core samples were provided by the IODP, funded by the U.S. National Science Foundation and participating countries. We are also grateful to R. Taylor, A. Michalik and C. Bristow for laboratory assistance and constructive discussions and to three anonymous reviewers whose comments greatly improved this manuscript. This study was supported by the University of Southampton in the form of a Mayflower Scholarship to G.E.J. I.B. acknowledges funding from an EU MARINEFF project (Interreg VA France-(Channel)-England Programme project #162). P.A.W. and A.J.C. acknowledge Royal Society funding including a Wolfson Merit Award to P.A.W.

Data availability

The data presented in this manuscript are available as a supplementary data table and.will also be deposited in the PANGAEA open access library.

583 **References**

584 Aarons, S.M., Blakowski, M.A., Aciego, S.M., Stevenson, E.I., Sims, K.W.W., Scott, S.R.,
585 Aarons, C., 2017. Geochemical characterization of critical dust source regions in the American
586 West. Geochimica Et Cosmochimica Acta 215, 141-161.

587 Abouchami, W., Näthe, K., Kumar, A., Galer, S.J.G., Jochum, K.P., Williams, E., Horbe, A.M.C.,
588 Rosa, J.W.C., Balsam, W., Adams, D., Mezger, K., Andreae, M.O., 2013. Geochemical and
589 isotopic characterization of the Bodélé Depression dust source and implications for transatlantic
590 dust transport to the Amazon Basin. Earth and Planetary Science Letters 380, 112-123.

591 Abouchami, W., Zabel, M., 2003. Climate forcing of the Pb isotope record of terrigenous input
592 into the Equatorial Atlantic. Earth and Planetary Science Letters 213, 221-234.

593 Ahn, J., Brook, E.J., Mitchell, L., Rosen, J., McConnell, J.R., Taylor, K., Etheridge, D., Rubino,
594 M., 2012. Atmospheric CO2 over the last 1000 years: A high-resolution record from the West
595 Antarctic Ice Sheet (WAIS) Divide ice core. Global Biogeochemical Cycles 26.

596 Ault, T.R., Mankin, J.S., Cook, B.I., Smerdon, J.E., 2016. Relative impacts of mitigation,
597 temperature, and precipitation on 21st-century megadrought risk in the American Southwest.
598 Science Advances 2.

599 Bailey, I., Foster, G.L., Wilson, P.A., Jovane, L., Storey, C.D., Trueman, C.N., Becker, J., 2012.
600 Flux and provenance of ice-rafted debris in the earliest Pleistocene sub-polar North Atlantic
601 Ocean comparable to the last glacial maximum. Earth and Planetary Science Letters 341-344,
602 222-233.

603 Baldridge, W.S., 2004. Geology of the American Southwest: A Journey through Two Billion
604 years of Plate-Tectonic History. Cambridge University Press, United Kingdom.

605 Balling, R.C., Goodrich, G.B., 2010. INCREASING DROUGHT IN THE AMERICAN
606 SOUTHWEST? A CONTINENTAL PERSPECTIVE USING A SPATIAL ANALYTICAL
607 EVALUATION OF RECENT TRENDS. Physical Geography 31, 293-306.

608 Bayon, G., German, C.R., Boella, R.M., Milton, J.A., Taylor, R.N., Nesbitt, R.W., 2002. An
609 improved method for extracting marine sediment fractions and its application to Sr and Nd
610 isotopic analysis. Chemical Geology 187, 179-199.

611 Behl, R.J., 1995. Sedimentary facies and sedimentology of the late Quaternary Santa Barbara
612 Basin, Site 893. Proceedings of the Ocean Drilling Program; Scientific Results 146, 295-308.

613 Betzer, P.R., Carder, K.L., Duce, R.A., Merrill, J.T., Tindale, N.W., Uematsu, M., Costello, D.K.,
614 Young, R.W., Feely, R.A., Breland, J.A., Bernstein, R.E., Greco, A.M., 1988. Long-range
615 transport of giant mineral aerosol particles. Nature 336, 568-571.

616 Bozlaker, A., Prospero, J.M., Price, J., Chellam, S., 2018. Linking Barbados Mineral Dust
617 Aerosols to North African Sources Using Elemental Composition and Radiogenic Sr, Nd, and Pb
618 Isotope Signatures. Journal of Geophysical Research: Atmospheres 123, 1384-1400.

619 Cayan, D.R., Das, T., Pierce, D.W., Barnett, T.P., Tyree, M., Gershunov, A., 2010. Future
620 dryness in the southwest US and the hydrology of the early 21st century drought. Proceedings
621 of the National Academy of Sciences of the United States of America 107, 21271-21276.

622 Chen, J., Li, G.J., Yang, J.D., Rao, W.B., Lu, H.Y., Balsam, W., Sun, Y.B., Ji, J.F., 2007. Nd and
623 Sr isotopic characteristics of Chinese deserts: Implications for the provenances of Asian dust.
624 Geochimica Et Cosmochimica Acta 71, 3904-3914.

625 Cole, J.M., Goldstein, S.L., Demenocal, P.B., Hemming, S.R., Grousset, F.E., 2009. Contrasting
626 compositions of Saharan dust in the eastern Atlantic Ocean during the last deglaciation and
627 African Humid Period. Earth and Planetary Science Letters 278, 257-266.

628 Conil, S., Hall, A., 2006. Local Regimes of Atmospheric Variability: A Case Study of Southern
629 California. Journal of Climate 19, 4308-4325.

630 Cook, B.I., Ault, T.R., Smerdon, J.E., 2015. Unprecedented 21st century drought risk in the
631 American Southwest and Central Plains. Sci. Adv 1, e1400082.

632 Cook, B.I., Smerdon, J.E., Seager, R., Cook, E.R., 2014. Pan-Continental Droughts in North
633 America over the Last Millennium. Journal of Climate 27, 383-397.

634 Cook, E.R., Seager, R., Cane, M.A., Stahle, D.W., 2007. North American drought:
635 Reconstructions, causes, and consequences. Earth-Science Reviews 81, 93-134.

636 Creamean, J.M., Spackman, J.R., Davis, S.M., White, A.B., 2014. Climatology of long-range
637 transported Asian dust along the West Coast of the United States. Journal of Geophysical
638 Research: Atmospheres 119, 2014JD021694.

639 Dasch, E.J., 1969. Strontium isotopes in weathering profiles, deep-sea sediments, and
640 sedimentary rocks. Geochimica et Cosmochimica Acta 33, 1521-1552.

641 de la Vega, E., Chalk, T.B., Wilson, P.A., Bysani, R.P., Foster, G.L., 2020. Atmospheric CO2
642 during the Mid-Piacenzian Warm Period and the M2 glaciation. Scientific Reports 10, 11002.

643 Feakins, S.J., Kirby, M.E., Cheetham, M.I., Ibarra, Y., Zimmerman, S.R.H., 2014. Fluctuation in
644 leaf wax D/H ratio from a southern California lake records significant variability in isotopes in
645 precipitation during the late Holocene. Organic Geochemistry 66, 48-59.

646 Feng, J.L., Zhu, L.P., Zhen, X.L., Hu, Z.G., 2009. Grain size effect on Sr and Nd isotopic
647 compositions in eolian dust: Implications for tracing dust provenance and Nd model age.
648 Geochemical Journal 43, 123-131.

649 Ginoux, P., Prospero, J.M., Gill, T.E., Hsu, N.C., Zhao, M., 2012. Global-scale attribution of
650 anthropogenic and natural dust sources and their emission rates based on MODIS Deep Blue
651 aerosol products. Reviews of Geophysics 50, RG3005.

652 Griggs, G.B., Hein, J.R., 1980. Sources, Dispersal, and Clay Mineral Composition of Fine-
653 Grained Sediment off Central and Northern California. The Journal of Geology 88, 541-566.

654 Hand, J.L., Gill, T.E., Schichtel, B.A., 2017. Spatial and seasonal variability in fine mineral dust
655 and coarse aerosol mass at remote sites across the United States. Journal of Geophysical
656 Research: Atmospheres 122, 3080-3097.

657 Hart, S.R., 1984. A large-scale isotope anomaly in the Southern Hemisphere mantle. Nature
658 309, 753-757.

659 Hoell, A., Funk, C., Barlow, M., 2014. The regional forcing of Northern hemisphere drought
660 during recent warm tropical west Pacific Ocean La Nina events. Climate Dynamics 42, 3289-

661 3311.

662 Hughes, M., Hall, A., 2010. Local and synoptic mechanisms causing Southern California's
663 Santa Ana winds. Climate Dynamics 34, 847-857.

664 Hyeong, K., Kim, J., Pettke, T., Yoo, C.M., Hur, S.-d., 2011. Lead, Nd and Sr isotope records of
665 pelagic dust: Source indication versus the effects of dust extraction procedures and authigenic
666 mineral growth. Chemical Geology 286, 240-251.

667 Inman, D.L., Jenkins, S.A., 1999. Climate Change and the Episodicity of Sediment Flux of Small
668 California Rivers. The Journal of Geology 107, 251-270.

669 Jacobsen, S.B., Wasserburg, G.J., 1980. SM-ND ISOTOPIC EVOLUTION OF CHONDRITES.
670 Earth and Planetary Science Letters 50, 139-155.

671 Jennings, C.W., Strand, R.G., 1981. Geologic Map of California, 5th ed.

672 Jewell, A.M., Drake, N., Crocker, A.J., Bakker, N.L., Kunkelova, T., Bristow, C.S., Cooper, M.J.,
673 Milton, J.A., Breeze, P.S., Wilson, P.A., 2021. Three North African dust source areas and their
674 geochemical fingerprint. Earth and Planetary Science Letters, 116645.

675 Johnson, C.M., O'Neil, J.R., 1984. Triple junction magmatism: a geochemical study of Neogene
676 volcanic rocks in western California. Earth and Planetary Science Letters 71, 241-262.

677 Jones, C.E., Halliday, A.N., Rea, D.K., Owen, R.M., 2000. Eolian inputs of lead to the North
678 Pacific. Geochimica et Cosmochimica Acta 64, 1405-1416.

679 Just, J., Heslop, D., von Dobeneck, T., Bickert, T., Dekkers, M.J., Frederichs, T., Meyer, I.,
680 Zabel, M., 2012. Multiproxy characterization and budgeting of terrigenous end-members at the
681 NW African continental margin. Geochemistry Geophysics Geosystems 13.

682 Kanayama, S., Yabuki, S., Zeng, F., Liu, M., Shen, Z.-z., Liu, L., Yanagisawa, F., Abe, O., 2005.
683 Size-dependent geochemical characteristics of Asian dust - Sr and Nd isotope compositions as
684 tracers for source identification. Journal of the Meteorological Society of Japan 83, 107-120.

685 Keeling, C.D., Piper, S.C., Bacastow, R.B., Wahlen, M., Whorf, T.P., Heimann, M., Meijer, H.A.,
686 2001. Exchanges of atmospheric CO2 and 13CO2 with the terrestrial biosphere and oceans
687 from 1978 to 2000. Scripps Institution of Oceanography, San Diego.

688 Kennett, J.P., Baldauf, J.G., Shipboard Scientific Party, 1994. Visual core description from ODP
689 Hole 143-893B.

690 Kumar, A., Abouchami, W., Galer, S.J.G., Garrison, V.H., Williams, E., Andreae, M.O., 2014. A
691 radiogenic isotope tracer study of transatlantic dust transport from Africa to the Caribbean.
692 Atmospheric Environment 82, 130-143.

693 Kumar, A., Abouchami, W., Galer, S.J.G., Singh, S.P., Fomba, K.W., Prospero, J.M., Andreae,
694 M.O., 2018. Seasonal radiogenic isotopic variability of the African dust outflow to the tropical
695 Atlantic Ocean and across to the Caribbean. Earth and Planetary Science Letters 487, 94-105.

696 Lang, D.C., Bailey, I., Wilson, P.A., Beer, C.J., Bolton, C.T., Friedrich, O., Newsam, C.,
697 Spencer, M.R., Gutjahr, M., Foster, G.L., Cooper, M.J., Milton, J.A., 2014. The transition on
698 North America from the warm humid Pliocene to the glaciated Quaternary traced by eolian dust
699 deposition at a benchmark North Atlantic Ocean drill site. Quaternary Science Reviews 93, 125-

700 141.

701 Larrasoana, J.C., Roberts, A.P., Rohling, E.J., Winklhofer, M., Wehausen, R., 2003. Three
702 million years of monsoon variability over the northern Sahara. Climate Dynamics 21, 689-698.

703 Lyle, M., Koizumi, I., Richter, C., Shipboard Scientific Party, 1997. Visual core description from
704 ODP Hole 167-1015B.

705 MacDonald, G.M., Stahle, D.W., Diaz, J.V., Beer, N., Busby, S.J., Cerano-Paredes, J., Cole,
706 J.E., Cook, E.R., Endfield, G., Gutierrez-Garcia, G., Hall, B., Magan, V., Meko, D.M., Méndez-
707 Pérez, M., Sauchyn, D.J., Watson, E., Woodhouse, C.A., 2008. Climate Warming and 21st-
708 Century Drought in Southwestern North America. Eos, Transactions American Geophysical
709 Union 89, 82-82.

710 Mahowald, N.M., Muhs, D.R., Levis, S., Rasch, P.J., Yoshioka, M., Zender, C.S., Luo, C., 2006.
711 Change in atmospheric mineral aerosols in response to climate: Last glacial period,
712 preindustrial, modern, and doubled carbon dioxide climates. Journal of Geophysical Research:
713 Atmospheres 111, n/a-n/a.

714 Marsaglia, K.M., Rimkus, K.C., Behl, R.J., 1995. Provenance of sand deposited in the Santa
715 Barbara Basin at Site 893 during the last 155,000 years. Proceedings of the Ocean Drilling
716 Program; Scientific Results 146, 61-75.

717 McKendry, I.G., Strawbridge, K.B., O'Neill, N.T., Macdonald, A.M., Liu, P.S.K., Leaitch, W.R.,
718 Anlauf, K.G., Jaegle, L., Fairlie, T.D., Westphal, D.L., 2007. Trans-Pacific transport of Saharan
719 dust to western North America: A case study. Journal of Geophysical Research: Atmospheres
720 112.

721 McManus, D.A., Burns, R.E., von der Borch, C.C., Goll, R.M., Milow, E.D., Olsson, R.K., Vallier,
722 T., Weser, O., 1970. Site 32. Affiliation (analytic): Univ. Wash., Seattle, WA 5, 15.

723 Medellín--Azuara, J., MacEwan, D., Howitt, R.E., Sumner, D.A., Lund, J.R., 2016. Economic
724 Impacts of the 2016 California Drought for Agriculture, p. 17.

725 Meinshausen, M., Smith, S.J., Calvin, K., Daniel, J.S., Kainuma, M.L.T., Lamarque, J.F.,
726 Matsumoto, K., Montzka, S.A., Raper, S.C.B., Riahi, K., Thomson, A., Velders, G.J.M., van
727 Vuuren, D.P.P., 2011. The RCP greenhouse gas concentrations and their extensions from 1765
728 to 2300. Climatic Change 109.

729 Meyer, I., Davies, G.R., Stuut, J.-B.W., 2011. Grain size control on Sr-Nd isotope provenance
730 studies and impact on paleoclimate reconstructions: An example from deep-sea sediments
731 offshore NW Africa. Geochemistry, Geophysics, Geosystems 12.

732 Muhs, D.R., Budahn, J., Reheis, M., Beann, J., Skipp, G., Fisher, E., 2007. Airborne dust
733 transport to the eastern Pacific Ocean off southern California: Evidence from San Clemente
734 Island. Journal of Geophysical Research-Atmospheres 112.

735 Muhs, D.R., Budahn, J.R., Johnson, D.L., Reheis, M., Beann, J., Skipp, G., Fisher, E., Jones,
736 J.A., 2008. Geochemical evidence for airborne dust additions to soils in Channel Islands
737 National Park, California. Geological Society of America Bulletin 120, 106-126.

738 Nakai, S., Halliday, A.N., Rea, D.K., 1993. PROVENANCE OF DUST IN THE PACIFIC-OCEAN.
739 Earth and Planetary Science Letters 119, 143-157.

740 Napier, T.J., Hendy, I.L., Fahnestock, M.F., Bryce, J.G., 2020. Provenance of detrital sediments
741 in Santa Barbara Basin, California, USA: Changes in source contributions between the Last
742 Glacial Maximum and Holocene. GSA Bulletin 132, 65-84.

743 NASA, 2002. Dusty Skies over Southern California

744 Nizou, J., Hanebuth, T.J.J., Vogt, C., 2011. Deciphering signals of late Holocene fluvial and
745 aeolian supply from a shelf sediment depocentre off Senegal (north-west Africa). Journal of
746 Quaternary Science 26, 411-421.

747 Perry, K.D., Cahill, T.A., Eldred, R.A., Dutcher, D.D., Gill, T.E., 1997. Long-range transport of
748 North African dust to the eastern United States. Journal of Geophysical Research: Atmospheres
749 102, 11225-11238.

750 Pettke, T., Halliday, A.N., Hall, C.M., Rea, D.K., 2000. Dust production and deposition in Asia
751 and the north Pacific Ocean over the past 12 Myr. Earth and Planetary Science Letters 178,
752 397-413.

753 Pourmand, A., Prospero, J.M., Sharifi, A., 2014. Geochemical fingerprinting of trans-Atlantic
754 African dust based on radiogenic Sr-Nd-Hf isotopes and rare earth element anomalies. Geology
755 42, 675-678.

756 Povea, P., Cacho, I., Moreno, A., Menendez, M., Mendez, F.J., 2015. A new procedure for the
757 lithic fraction characterization in marine sediments from high productivity areas: Optimization of
758 analytical and statistical procedures. Limnology and Oceanography-Methods 13, 127-137.

759 Prospero, J.M., Ginoux, P., Torres, O., Nicholson, S.E., Gill, T.E., 2002. Environmental
760 characterization of global sources of atmospheric soil dust identified with the NIMBUS 7 Total
761 Ozone Mapping Spectrometer (TOMS) absorbing aerosol product. Reviews of Geophysics 40,
762 1002.

763 Pye, K., 1987a. Chapter 3 - DUST ENTRAINMENT, TRANSPORT AND DEPOSITION, Aeolian
764 Dust and Dust Deposits. Academic Press, pp. 29-62.

765 Pye, K., 1987b. Chapter 4 - DUST SOURCES, SINKS AND RATES OF DEPOSITION, Aeolian
766 Dust and Dust Deposits. Academic Press, pp. 63-91.

767 Rea, D.K., 1994. The paleoclimatic record provided by eolian deposition in the deep sea: The
768 geologic history of wind. Reviews of Geophysics 32, 159-195.

769 Reheis, M.C., Goodmacher, J.C., Harden, J.W., McFadden, L.D., Rockwell, T.K., Shroba, R.R.,
770 Sowers, J.M., Taylor, E.M., 1995. QUATERNARY SOILS AND DUST DEPOSITION IN
771 SOUTHERN NEVADA AND CALIFORNIA. Geological Society of America Bulletin 107, 1003-
772 1022.

773 Reynolds, R.L., Reheis, M., Yount, J., Lamothe, P., 2006. Composition of aeolian dust in natural
774 traps on isolated surfaces of the central Mojave Desert—Insights to mixing, sources, and
775 nutrient inputs. Journal of Arid Environments 66, 42-61.

776 Rosenbauer, R.J., Foxgrover, A.C., Hein, J.R., Swarzenski, P.W., 2013. A Sr–Nd isotopic study
777 of sand-sized sediment provenance and transport for the San Francisco Bay coastal system.
778 Marine Geology 345, 143-153.

779 Routson, C.C., Overpeck, J.T., Woodhouse, C.A., Kenney, W.F., 2016. Three Millennia of

780 Southwestern North American Dustiness and Future Implications. Plos One 11.

781 Salzer, M.W., Kipfmueller, K.F., 2005. Reconstructed temperature and precipitation on a
782 millennial timescale from tree-rings in the Southern Colorado Plateau, USA. Climatic Change
783 70, 465-487.

784 Schwalbach, J.R., Gorsline, D.S., 1985. HOLOCENE SEDIMENT BUDGETS FOR THE
785 BASINS OF THE CALIFORNIA CONTINENTAL BORDERLAND. Journal of Sedimentary
786 Petrology 55, 829-842.

787 Seager, R., Ting, M., Held, I., Kushnir, Y., Lu, J., Vecchi, G., Huang, H.-P., Harnik, N., Leetmaa,
788 A., Lau, N.-C., Li, C., Velez, J., Naik, N., 2007. Model Projections of an Imminent Transition to a
789 More Arid Climate in Southwestern North America. Science 316, 1181-1184.

790 Seo, I., Lee, Y.I., Kim, W., Yoo, C.M., Hyeong, K., 2015. Movement of the Intertropical
791 Convergence Zone during the mid-pleistocene transition and the response of atmospheric and
792 surface ocean circulations in the central equatorial Pacific. Geochemistry Geophysics
793 Geosystems 16, 3973-3981.

794 Seo, I., Lee, Y.I., Yoo, C.M., Kim, H.J., Hyeong, K., 2014. Sr-Nd isotope composition and clay
795 mineral assemblages in eolian dust from the central Philippine Sea over the last 600 kyr:
796 Implications for the transport mechanism of Asian dust. Journal of Geophysical Research:
797 Atmospheres 119, 2014JD022025.

798 Skonieczny, C., Bory, A., Bout-Roumazeilles, V., Abouchami, W., Galer, S.J.G., Crosta, X.,
799 Diallo, A., Ndiaye, T., 2013. A three-year time series of mineral dust deposits on the West
800 African margin: Sedimentological and geochemical signatures and implications for interpretation
801 of marine paleo-dust records. Earth and Planetary Science Letters 364, 145-156.

802 Skonieczny, C., Bory, A., Bout-Roumazeilles, V., Abouchami, W., Galer, S.J.G., Crosta, X.,
803 Stuut, J.B., Meyer, I., Chiapello, I., Podvin, T., Chatenet, B., Diallo, A., Ndiaye, T., 2011a. The
804 7–13 March 2006 major Saharan outbreak: Multiproxy characterization of mineral dust
805 deposited on the West African margin. Journal of Geophysical Research: Atmospheres 116.

806 Skonieczny, C., Bory, A., Bout-Roumazeilles, V., Abouchami, W., Galer, S.J.G., Crosta, X.,
807 Stuut, J.B., Meyer, I., Chiapello, I., Podvin, T., Chatenet, B., Diallo, A., Ndiaye, T., 2011b. The
808 7–13 March 2006 major Saharan outbreak: Multiproxy characterization of mineral dust
809 deposited on the West African margin. Journal of Geophysical Research: Atmospheres 116.

810 Stancin, A.M., Gleason, J.D., Rea, D.K., Owen, R.M., Moore, T.C., Blum, J.D., Hovan, S.A.,
811 2006. Radiogenic isotopic mapping of late Cenozoic eolian and hernipelagic sediment
812 distribution in the east-central Pacific. Earth and Planetary Science Letters 248, 840-850.

813 Sun, J.M., Zhu, X.K., 2010. Temporal variations in Pb isotopes and trace element
814 concentrations within Chinese eolian deposits during the past 8 Ma: Implications for provenance
815 change. Earth and Planetary Science Letters 290, 438-447.

816 Super, J.R., Thomas, E., Pagani, M., Huber, M., O'Brien, C., Hull, P.M., 2018. North Atlantic
817 temperature and pCO2 coupling in the early-middle Miocene. Geology 46, 519-522.

818 Tanaka, T., Togashi, S., Kamioka, H., Amakawa, H., Kagami, H., Hamamoto, T., Yuhara, M.,
819 Orihashi, Y., Yoneda, S., Shimizu, H., Kunimaru, T., Takahashi, K., Yanagi, T., Nakano, T.,
820 Fujimaki, H., Shinjo, R., Asahara, Y., Tanimizu, M., Dragusanu, C., 2000. JNdi-1: a neodymium

821 isotopic reference in consistency with LaJolla neodymium. Chemical Geology 168, 279-281.

822 Taylor, R.N., Ishizuka, O., Michalik, A., Milton, J.A., Croudace, I.W., 2015. Evaluating the
823 precision of Pb isotope measurement by mass spectrometry. Journal of Analytical Atomic
824 Spectrometry 30, 198-213.

825 Tchakerian, V.P., Lancaster, N., 2002. Late quaternary arid/humid cycles in the Mojave Desert
826 and western Great Basin of North America. Quaternary Science Reviews 21, 799-810.

827 Tiedemann, R., Sarnthein, M., Shackleton, N.J., 1994. Astronomic timescale for the Pliocene
828 Atlantic δ18O and dust flux records of Ocean Drilling Program Site 659. Paleoceanography 9,
829 619-638.

830 Toomey, M., 2010. KML to SHP conversion using kml_shapefile, 1.2.0.0 ed, MATLAB Central
831 File Exchange.

832 Uno, I., Eguchi, K., Yumimoto, K., Liu, Z., Hara, Y., Sugimoto, N., Shimizu, A., Takemura, T.,
833 2011. Large Asian dust layers continuously reached North America in April 2010. Atmos. Chem.
834 Phys. 11, 7333-7341.

835 Urban, F.E., Goldstein, H.L., Fulton, R., Reynolds, R.L., 2018. Unseen Dust Emission and
836 Global Dust Abundance: Documenting Dust Emission from the Mojave Desert (USA) by Daily
837 Remote Camera Imagery and Wind-Erosion Measurements. Journal of Geophysical Research-
838 Atmospheres 123, 8735-8753.

839 van der Does, M., Knippertz, P., Zschenderlein, P., Giles Harrison, R., Stuut, J.-B.W., 2018a.
840 The mysterious long-range transport of giant mineral dust particles. Science Advances 4.

841 van der Does, M., Pourmand, A., Sharifi, A., Stuut, J.-B.W., 2018b. North African mineral dust
842 across the tropical Atlantic Ocean: Insights from dust particle size, radiogenic Sr-Nd-Hf isotopes
843 and rare earth elements (REE). Aeolian Research 33, 106-116.

844 Vance, D., Thirlwall, M., 2002. An assessment of mass discrimination in MC-ICPMS using Nd
845 isotopes. Chemical Geology 185, 227-240.

846 VanCuren, R.A., Cahill, T.A., 2002. Asian aerosols in North America: Frequency and
847 concentration of fine dust. Journal of Geophysical Research: Atmospheres 107, AAC 19-11-
848 AAC 19-16.

849 Walter, H.J., Hegner, E., Diekmann, B., Kuhn, G., Rutgers van der loeff, M.M., 2000.
850 Provenance and transport of terrigenous sediment in the south Atlantic Ocean and their
851 relations to glacial and interglacial cycles: Nd and Sr isotopic evidence. Geochimica et
852 Cosmochimica Acta 64, 3813-3827.

853 Weigand, P., 1993. Geochemistry and Origin of Middle Miocene Volcanic Rocks from Santa
854 Cruz and Anacapa Islands, Southern California Borderland. Santa Barbara Museum of Natural
855 History, Santa Barbara, CA.

856 Weigand, P.W., Savage, K.L., 1999. Summary of the Miocene Igneous rocks of the Channel
857 Islands, Southern California, in: Browne, D.R.H., Chaney, H., Mitchell, eds. (Eds.), Fifth
858 Californian Islands Symposium.

859 Wu, F., Ho, S.S.H., Sun, Q.L., Ip, S.H.S., 2011. Provenance of Chinese Loess: Evidence from
860 Stable Lead Isotope. Terr. Atmos. Ocean. Sci. 22, 305-314.

861 Xie, R.F.C., Marcantonio, F., 2012. Deglacial dust provenance changes in the Eastern
862 Equatorial Pacific and implications for ITCZ movement. Earth and Planetary Science Letters
863 317, 386-395.

864 Zeng, F., Liang, M., Peng, S., Yu, D., Xiang, S., 2015. Sr-Nd-Pb Isotopic Compositions of the
865 Neogene Eolian Deposits in the Xining Basin and Implications for Their Dust Sources. Journal
866 of Earth Science 26, 669-676.

867 Zhao, W., Sun, Y., Balsam, W., Zeng, L., Lu, H., Otgonbayar, K., Ji, J., 2015. Clay-sized Hf-Nd-
868 Sr isotopic composition of Mongolian dust as a fingerprint for regional to hemispherical
869 transport. Geophysical Research Letters 42, 5661-5669.

870